SIAM J. APPL. MATH.
Vol. 80, No. 6, pp. 2472–2495

AMPLITUDE BLOWUP IN RADIAL ISENTROPIC EULER FLOW*

HELGE KRISTIAN JENSSEN† AND CHARIS TSIKKOU‡

Abstract. We show that the compressible Euler system for isentropic gas flow admits unbounded solutions. The examples are radial flows of similarity type and describe a spherically symmetric and continuous wave moving toward the origin. At time of focusing, both the density and the velocity become unbounded at the origin. This is followed by an expanding shock wave which slows down as it interacts with the incoming flow. While unbounded radial Euler flows have been known since the work of Guderley [*Luftfahrtforschung*, 19 (1942), pp. 302–311], those are at the borderline of the regime covered by the Euler model: The upstream pressure field vanishes identically (either because of vanishing temperature or vanishing density there). In contrast, the solutions we build exhibit an everywhere strictly positive pressure field, demonstrating that the geometric effect of wave focusing is strong enough on its own to drive the primary flow variables to infinity.

Key words. compressible fluid flow, multi-d isentropic Euler system, similarity solutions, radial symmetry, unbounded solutions

AMS subject classifications. 35L45, 35L67, 76N10, 35Q31

DOI. 10.1137/20M1340241

1. Introduction.

We consider inviscid isentropic flow in $n = 2$ or 3 space dimensions as described by the compressible Euler equations which express conservation of mass and linear momentum:

$$\rho_t + \mathrm{div}_{\mathbf{x}}(\rho \mathbf{u}) = 0, \tag{1.1}$$

$$(\rho \mathbf{u})_t + \mathrm{div}_x[\rho \mathbf{u} \otimes \mathbf{u}] + \mathrm{grad}_{\mathbf{x}}\, p = 0. \tag{1.2}$$

The independent variables are time t and position $\mathbf{x} \in \mathbb{R}^n$, and the primary dependent variables are the density ρ and the fluid velocity $\mathbf{u}$. In isentropic flow the pressure p is given as

$$p(\rho) = a^2 \rho^\gamma \qquad (a > 0,\ \gamma > 1 \text{ constants}). \tag{1.3}$$

It is well known that even initially smooth flows in general suffer gradient blowup (shock formation) [6]. In this work, we are concerned with the much less studied phenomenon of *amplitude* blowup: For hyperbolic equations in several space dimensions, the phenomenon of wave focusing may generate unbounded amplitudes (e.g., for the linear wave equation).

In this setting it is natural to restrict attention to solutions with symmetry. We shall consider so-called *radial* flows in which the variables depend on position only through the distance $r = |\mathbf{x}|$ to the origin, and in addition the velocity field is purely

*Received by the editors May 26, 2020; accepted for publication (in revised form) September 22, 2020; published electronically December 1, 2020.
https://doi.org/10.1137/20M1340241
Funding: The work of the first author was supported by the NSF through grant DMS-1813283. The work of the second author was supported by the NSF through grant DMS-1714912.

†Department of Mathematics, Penn State University, University Park, State College, PA 16802 USA (jenssen@math.psu.edu).
‡Department of Mathematics, West Virginia University, Morgantown, WV 26506 USA (tsikkou@math.wvu.edu).

radial: $\mathbf{u} = u\frac{\mathbf{x}}{r}$. Under these assumptions (1.1)–(1.2) reduce to

$$(r^m\rho)_t + (r^m\rho u)_r = 0, \tag{1.4}$$

$$(r^m\rho u)_t + \left(r^m(\rho u^2 + p)\right)_r = mr^{m-1}p. \tag{1.5}$$

For smooth flows this reduces further to

$$\rho_t + u\rho_r + \rho(u_r + \tfrac{mu}{r}) = 0, \tag{1.6}$$

$$u_t + uu_r + \tfrac{1}{\rho}p_r = 0, \tag{1.7}$$

where $\rho = \rho(t, r)$, $u = u(t, r)$, and $m = n - 1$.

In (1.6)–(1.7) the multi-d aspect enters only through the geometric source term $\frac{m\rho u}{r}$ in (1.6). As this term contains the unbounded factor $\frac{1}{r}$, it appears reasonable that the multi-d Euler system would admit unbounded solutions. For example, one could reasonably expect a scenario in which the geometric effect of focusing (as encoded in the term $\frac{m\rho u}{r}$) would be sufficiently strong to generate infinite amplitudes in a radially converging flow.

On the other hand, the appearance of unbounded amplitudes of primary flow variables raises issues about the physicality of the model. One might ask if there could be a mechanism whereby the Euler system could "save itself" from such behavior. One possibility would be that the upstream pressure in the fluid near the center of motion could provide sufficient counterpressure to somehow prevent actual blowup.

As it turns out, there is a well-studied class of Euler solutions that *do* exhibit unbounded amplitudes. These are the so-called *Guderley solutions*, which provide one of the few instances where multi-d, compressible flows can be studied in detail. They have received considerable attention in the literature of inertial confinement fusion; see [1, 7, 13]. The flows in question are similarity solutions (see below) of the Euler system for an ideal, polytropic fluid with equation of state $p = R\rho T$. The solutions solve the full model (including energy conservation) and were first considered by Guderley [8]. However, they are also—*regardless of their blowup behavior*—at the borderline of where the Euler model can be expected to be physically valid.

To explain this, we recall [10, 12] that Guderley solutions involve a single, converging spherical (or cylindrical) shock wave which invades a quiescent fluid near the origin, the fluid being at rest and at constant density and pressure there. The shock collapses on the origin with infinite speed and generates an expanding shock wave which then propagates outward as it interacts with the still-incoming flow. At time of collapse, the velocity, pressure, sound speed, and temperature (but not the density) attain infinite values at the center of motion. However, as pointed out in [12], in order to provide an exact solution of the Euler system, the sound speed within the quiescent region must necessarily vanish. For the ideal gas case under consideration, this means that there is no upstream counterpressure due to a vanishing temperature field there. Thus, the flow regime exhibited by these solutions is a borderline case where the Euler model is of questionable physicality.

In fact, it is reasonable to ask if it is precisely this absence of a counterpressure which is responsible for the blowup, the idea being that the lack of counterpressure would facilitate unbounded growth in shock speed, with concomitant increases of amplitudes in the immediate wake of the converging shock wave. We stress that Guderley solutions of the type described can be shown to be exact weak solutions of the full Euler system: Despite the presence of infinite values of the primary flow variables, they satisfy the weak form of the full, multi-d Euler system, [10].

The upshot is that, although Guderley solutions provide examples of unbounded, genuine weak solutions to the Euler system, they fail to settle the issue of whether amplitude blowup is possible in the presence of an everywhere positive pressure field. *The goal of the present work is to demonstrate that this* is *possible and that, notwithstanding unbounded amplitudes, such solutions provide genuine weak solutions of the multi-d Euler system (see Definition* 5.1*).*

We shall carry out the analysis for the simplified isentropic model (1.1)–(1.2) and (1.3) with $\gamma > 1$. While we expect that the same conclusion holds for the full Euler model, it is of interest to establish this type of behavior separately for the isentropic model. Indeed, this is the only Euler model for which an existence theory for radial flows is currently available (see discussion below). On the other hand, the latter theory is based on the method of compensated compactness and does not provide (or has not yet provided) information about the possibility of amplitude blowup in radial flows.

The authors have recently established the same conclusion (i.e., possibility of blowup in absence of zero-pressure regions) for the *isothermal* model: (1.1)–(1.2) and (1.3) with $\gamma = 1$; see [11]. That work provided the existence of radial similarity solutions in which an incoming wave approaches the origin in the presence of a strictly positive upstream pressure field, collapses at the origin, and gives rise to an expanding shock wave. There are two notable differences between the isothermal solutions constructed in [11] and the Guderley solutions described above. First, the incoming wave is continuous (possibly containing a weak discontinuity, i.e., a jump in its gradient), and, second, it is only the density field (and not the velocity field) which suffers blowup at time of collapse. The isentropic blowup solutions we construct below exhibit a mixture of these behaviors: The incoming wave will again be continuous, but both the density and the velocity suffer blowup at collapse.

It turns out that the analysis of the isothermal model in [11] is rather different and significantly simpler compared to the isentropic model or the full model. On the other hand, for the isentropic case considered here, we can make use of results established in earlier analyses. Our reference for these results (one among several possibilities) is the comprehensive work of Lazarus [12], which built on earlier joint work with Richtmyer (see references in [12]).

1.1. Similarity variables and similarity ODEs. Before formulating our main result, we introduce the type of similarity solutions to be utilized to give examples of isentropic amplitude blowup. The solutions are globally defined on all of space-time and may be described as "converging-diverging flows" in which the blowup occurs at, and only at, the origin at the time of collapse. Due to invariance under time translation, we are free to let $t = 0$ be the time of collapse, a choice which is built into the type of solutions we consider.

It is well known that the Euler system admits similarity solutions [5, 8, 15, 16]. Following [12], we introduce the similarity variables

(1.8)
$$x = \frac{t}{r^\lambda}, \qquad \rho(t,r) = r^\kappa R(x), \qquad u(t,r) = -\frac{r^{1-\lambda}}{\lambda}\frac{V(x)}{x}, \qquad c(t,r) = -\frac{r^{1-\lambda}}{\lambda}\frac{C(x)}{x},$$

where $\lambda > 1$ is the *similarity exponent* and the local sound speed c given by

$$c := \sqrt{p'(\rho)} = \sqrt{\gamma} a \rho^{\frac{\gamma-1}{2}}.$$

As $c \propto \rho^{\frac{\gamma-1}{2}}$, (1.8) is consistent only if

$$\kappa = -\frac{2(\lambda-1)}{\gamma-1}, \tag{1.9}$$

which is assumed from now on. Thus, $R(x)$ and $C(x)$ are related by

$$C^2(x) = \gamma a^2 \lambda^2 x^2 R^{\gamma-1}(x),$$

and the density field takes the form

$$\rho(t,r) = r^\kappa R(x) = r^\kappa \left[\frac{C(x)^2}{\gamma\lambda^2 a^2 x^2}\right]^{\frac{1}{\gamma-1}}, \qquad x = \frac{t}{r^\lambda}. \tag{1.10}$$

Substitution of (1.8) into (1.6)–(1.7) yields the following similarity ODEs:

$$V'(x) = -\frac{1}{\lambda x}\frac{G(V(x),C(x),\lambda)}{D(V(x),C(x))}, \tag{1.11}$$

$$C'(x) = -\frac{1}{\lambda x}\frac{F(V(x),C(x),\lambda)}{D(V(x),C(x))}, \tag{1.12}$$

where the polynomial functions D, F, and G are given by

$$D(V,C) = (1+V)^2 - C^2, \tag{1.13}$$

$$G(V,C,\lambda) = C^2(nV-\kappa) - V(1+V)(\lambda+V), \tag{1.14}$$

$$F(V,C,\lambda) = C\left\{C^2 - k_1(1+V)^2 + k_2(1+V) - k_3\right\}, \tag{1.15}$$

where

$$k_1 = 1 + \tfrac{(n-1)(\gamma-1)}{2}, \qquad k_2 = \tfrac{(n-1)(\gamma-1)+(\gamma-3)(\lambda-1)}{2}, \qquad k_3 = \tfrac{(\gamma-1)(\lambda-1)}{2}.$$

For later reference, we note the symmetries

$$G(V,-C,\lambda) = G(V,C,\lambda), \qquad F(V,-C,\lambda) = -F(V,C,\lambda). \tag{1.16}$$

Combining (1.11) and (1.12) gives an autonomous ODE (no explicit x-dependence)

$$\frac{dC}{dV} = \frac{F(V,C,\lambda)}{G(V,C,\lambda)} \tag{1.17}$$

relating V and C along similarity solutions.

Equation (1.17) is of key importance: Trajectories of it will provide the various parts of the flows we seek. While (1.17) can be analyzed in some detail (e.g., its critical points, their locations and types, and their dependencies on n, γ, and λ), we have found it necessary to assume a technical "property (Π)" in order to generate flows in which the blowup leads to the generation of an expanding shock wave. This technical condition requires that the "Hugoniot locus" associated with a certain trajectory of (1.17) intersects a certain other trajectory of (1.17). The precise formulations of property (Π) is given in section 4.4.

Remark 1.1. We stress that numerical calculations clearly indicate that the property (Π) is satisfied for infinitely many solutions for each relevant choice of n, γ, λ. (See Main Result below and Remark 4.7 for details.) On the other hand, it appears challenging to provide an analytic proof of this.

Next we list five physically motivated properties to be satisfied by the flows we seek:

(A) The velocity at the center of motion vanishes: $u(t,0) = 0$ for all times $t \gtrless 0$.

(B) The density at the center of motion is finite and nonvanishing, except at time of collapse: $0 < \rho(t,0) < \infty$ for all times $t \gtrless 0$.

(C) At any fixed location away from the origin the density and velocity approach finite limits at the time of collapse; i.e., for each $r > 0$,

$$\lim_{t\to 0} u(t,r) \qquad \text{and} \qquad \lim_{t\to 0} \rho(t,r) \tag{1.18}$$

exist as finite numbers $u(0,r)$ and $\rho(0,r)$, respectively. Equivalently, $t \mapsto u(t,r)$ and $t \mapsto \rho(t,r)$ are continuous at $t = 0$ at each position $r > 0$.

(D) The density is everywhere strictly positive: $\rho(t,r) > 0$ for all $(t,r) \in \mathbb{R} \times \mathbb{R}^+$.

(E) The total energy density $\frac{1}{2}\rho|\mathbf{u}|^2 + \frac{a^2}{\gamma-1}\rho^\gamma$ belongs to $L^1_{loc}(\mathbb{R}^n)$ at all times.

We note that requirement (C) allows for the possibility that $\rho(0,r)$ and/or $u(0,r)$ blow up as $r \downarrow 0$; see (4.17)–(4.18) for the blowup profiles that obtain. Also, as discussed above, property (D) is central to the solutions we construct: For the isentropic model it implies that the pressure field is everywhere strictly positive.

Our main result is the following (where we slightly abuse notation by employing the same symbol for the density field in rectangular and radial coordinates).

Main Result. *Consider the isentropic Euler system* (1.1)–(1.2) *and* (1.3) *in space dimension $n = 2$ or $n = 3$, and consider radial similarity solutions of the form*

$$\rho(t,\mathbf{x}) := \rho(t,|\mathbf{x}|) \qquad \mathbf{u}(t,\mathbf{x}) := u(t,|\mathbf{x}|)\tfrac{\mathbf{x}}{|\mathbf{x}|}, \tag{1.19}$$

where $(\rho,u)(t,r)$ solves (1.4)–(1.5) *and are of the form* (1.8)*, with V and C solving* (1.11)–(1.12)*. Then for each $\gamma > 1$ there is a number $\hat\lambda = \hat\lambda(\gamma,n) > 1$ such that the following holds:*

1. *For each similarity exponent $\lambda \in (1,\hat\lambda)$ there are infinitely many radial similarity solutions $(\rho,u)(t,r)$ in which both the density and the velocity suffer amplitude blowup at the origin as $t \uparrow 0$.*
2. *Furthermore, each solution satisfying condition* (Π) *(see section* 4.4*) can be continued to all times $t > 0$ and contains an admissible, expanding shock wave emanating from the origin. These similarity solutions satisfy the properties* (A)–(E) *above. Finally, the pairs $(\rho(t,\mathbf{x}),\mathbf{u}(t,\mathbf{x}))$ defined by* (1.19) *are admissible weak solutions of the multi-d isentropic Euler system* (1.1)–(1.2) *according to Definition* 5.1 *below.*

We note that the similarity solutions described by the Main Result are defined globally on all of space-time. Also, the weak forms of (1.1) and (1.2) are formulated without any terms related to initial data; see (5.1)–(5.2). However, Definition 5.1 also requires that the conserved quantities map time continuously into $L^1_{loc}(\mathbb{R}^n_{\mathbf{x}})$. It follows from this that any weak solution will, when restricted to a time interval $[t_0,+\infty)$, also be a weak solution to the Cauchy problem with initial data $(\rho(t_0,\cdot),\mathbf{u}(t_0,\cdot))$ at time $t = t_0$.

The demonstration of the Main Result requires a rather detailed analysis of the critical points of the similarity ODE (1.17) and the Rankine–Hugoniot relations and admissibility conditions for the emerging shock wave. In particular, the shock will be compressive: The density of a fluid parcel increases as it passes through the shock surface.

We conclude with some comments about known existence results for radial Euler flows with "general" initial data. First, there is at present no general existence result available for the full, multi-d Euler system that guarantees global-in-time existence of radial solutions. Restricting to radial isentropic flows ($\gamma > 1$) the results in [2, 3, 4] provide existence of weak, finite energy solutions via the method of compensated compactness. Schrecker [14] has recently established that the solutions so obtained are weak solutions to the original, multi-d isentropic Euler system (1.1)–(1.2) on *all* of space (i.e., including the origin). These works provide weak solutions for general, finite energy data; however, they yield no information about the possibility/impossibility of amplitude blowup.

The rest of the paper is organized as follows. Section 2 records the Rankine–Hugoniot relations and the admissibility condition for shocks in similarity solutions. The construction of the radial similarity flows described in the Main Result is somewhat involved. We have found it convenient to first give an outline in section 3. This is followed by a detailed argument in section 4, including a precise formulation of condition (Π). (This analysis makes use of several technical results from [12].) Section 4.6 collects some additional properties (in particular, locally bounded total energy) of the constructed solutions, which are then used in section 5 to verify that they provide genuine, weak solutions to the multi-d isentropic Euler system, completing the demonstration of the Main Result. Finally, section 6 includes two observations about characteristics and particle trajectories for the constructed solutions. In particular, we argue that the type of amplitude blowup exhibited by these solutions can occur also in flows with finite total mass and energy.

2. Jump and entropy conditions for similarity shocks. Consider the radial isentropic Euler system (1.6)–(1.7) and (1.3), and assume that a discontinuity propagates along the path $r = \mathcal{R}(t)$. The Rankine–Hugoniot conditions are

$$\dot{\mathcal{R}}\big[\![\rho]\!\big] = \big[\![\rho u]\!\big] \qquad \text{and} \qquad \dot{\mathcal{R}}\big[\![\rho u]\!\big] = \big[\![\rho u^2 + a^2\rho^\gamma]\!\big], \tag{2.1}$$

where we use the convention that, for any quantity $q = q(t, r)$,

$$\big[\![q]\!\big] := q_+ - q_- \equiv q(t, \mathcal{R}(t)+) - q(t, \mathcal{R}(t)-),$$

where the subscript "$-$" denotes the value on the inside (i.e., closer to $r = 0$) of the discontinuity. The entropy conditions for 1-shocks and 2-shocks require that

$$u_- - c_- > \dot{\mathcal{R}} > u_+ - c_+ \qquad \text{and} \qquad u_- + c_- > \dot{\mathcal{R}} > u_+ + c_+, \tag{2.2}$$

respectively. We next specialize to "similarity shocks" propagating along $x \equiv \bar{x}$, i.e., along

$$r = \mathcal{R}(t) = (\tfrac{t}{\bar{x}})^{\frac{1}{\lambda}}. \tag{2.3}$$

With ρ, u, c as in (1.8), with the same values of γ and λ on each side of the shock, and with

$$W := 1 + V \qquad \text{and} \qquad \tilde{a}^2 := a^2\lambda^2\bar{x}^2,$$

the Rankine–Hugoniot conditions (2.1) take the form

$$\big[\![RW]\!\big] = 0 \qquad \text{and} \qquad \big[\![RW^2 + \tilde{a}^2 R^\gamma]\!\big] = 0, \tag{2.4}$$

where $[\![\cdot]\!]$ now denotes jump across $x = \bar{x}$. We note that the entropy condition for a

2-shock propagating along $x \equiv \bar{x}$, with $\bar{x} > 0$, takes the following form in terms of V and C:

$$-1 - V_- - C_- > 0 > -1 - V_+ - C_+. \tag{2.5}$$

The next result amounts to the fact that, with $\bar{x} > 0$ and (V_+, C_+) satisfying the last inequality in (2.5), there is a unique state (V_-, C_-) which connects to (V_+, C_+) through an entropy-admissible 2-shock across $x = \bar{x}$. This will be used to locate the expanding shock wave in the solutions described in the Main Result.

LEMMA 2.1. *Assume V_+, C_+ satisfy $-1 - V_+ < C_+ < 0$ and $\bar{x} > 0$. Then there is a unique pair (V_-, C_-) such that*

(a) *(V_-, C_-) and (V_+, C_+) satisfy the Rankine–Hugoniot conditions* (2.4)*;*

(b) *$-1 - V_- > C_-$.*

Proof. It is convenient to use the variables R and $W = 1 + V$. We first calculate R_+ from (1.10) (noting that $R_+ > 0$) and proceed to solve for R_-. Setting $M := R_+ W_+$ and defining the function $f(R) := M^2 R^{-1} + \tilde{a}^2 R^\gamma$, $(2.4)_1$ gives $R_- W_- = M$, while $(2.4)_2$ gives

$$f(R_-) = f(R_+). \tag{2.6}$$

It follows from the properties of f that (2.6) has a unique solution $R_- > 0$ ($R_- \neq R_+$) and that $R_\pm$ are located at opposite sides of the unique minimum point R_* of f, the latter being given by $R_*^{\gamma+1} = \frac{M^2}{\gamma \tilde{a}^2}$. W_- and C_-^2 are then determined from R_- by using $(2.4)_1$ and (1.10), respectively. Note that part (a) of the lemma is now satisfied by construction. However, C_- is so far only determined up to a sign, and it remains to verify that part (b) will be satisfied by appropriately choosing this sign. By assumption, we have $-W_+ < C_+ < 0$, so that $C_+^2 < W_+^2$, which is equivalent, via (1.10), to $R_+^{\gamma+1} < R_*^{\gamma+1}$. Thus, $R_+ < R_* < R_-$. In turn, the last inequality yields, again via (1.10), $W_-^2 < C_-^2$. Also, since $R_\pm > 0$, it follows from the assumption $W_+ > 0$ that $R_- W_- = M = R_+ W_+ > 0$, so that $W_- > 0$. We therefore have $0 < W_- < |C_-|$. Thus, (b) will be satisfied if and only if C_- is chosen negative. With this choice, we have identified unique values V_- and C_- so that (a) and (b) both hold. ∎

We note that the proof above establishes the inequality $R_+ < R_-$; this shows that admissibility implies that the shock is compressive.

3. Construction of converging-diverging flows: Outline. The goal is to construct particular solutions $(V(x), C(x))$ of (1.11)–(1.12) that give, via (1.8), unbounded solutions of the radial Euler system (1.6)–(1.7) and also satisfy the requirements (A)–(E). The details of the construction are somewhat involved, and we find it helpful to first give an outline in this section. In particular, we explain the property (Π) that we need to assume; this will be formulated precisely in the next section. From now on, we fix $n = 2$ or 3 and $\gamma > 1$.

We first formulate the requirements (A)–(D) in terms of the similarity variables (recall that $c \propto \rho^{\frac{\gamma-1}{2}}$, so that the conditions on ρ may be expressed in terms of C):

(A) $\lim_{x \to \pm\infty} \frac{V(x)}{|x|^{\frac{1}{\lambda}}} = 0$;

(B) $0 < \lim_{x \to \pm\infty} \frac{|C(x)|}{|x|^{\frac{1}{\lambda}}} < \infty$;

(C) the limits $\lim_{x \to 0} \frac{V(x)}{x}$ and $\lim_{x \to 0} \frac{C(x)}{x}$ both exist as finite numbers;

(D) $\frac{C(x)}{x} < 0$ for all $x \in \mathbb{R}$.

To build the relevant solutions of (1.11)–(1.12), we shall make use of particular trajectories of the autonomous ODE (1.17). This requires knowing the locations and types of its critical points, i.e., the points of intersection between the zero-level curves

$$\mathcal{F} := \{(V,C)\,|\,F(V,C)=0\} \qquad \text{and} \qquad \mathcal{G} := \{(V,C)\,|\,G(V,C)=0\}.$$

This analysis was carried out in detail by Lazarus [12], and we shall make use of those results. For this discussion it is convenient to define the "critical lines"

$$L_\pm := \{(V,C)\,|\,C=\pm(1+V)\}. \tag{3.1}$$

First, (1.17) has two critical points at infinity, namely,

$$P_{\pm\infty} := (V_*, \pm\infty), \quad \text{where } V_* := \tfrac{\kappa}{n} = -\tfrac{2(\lambda-1)}{n(\gamma-1)} \tag{3.2}$$

is the location of the vertical asymptote of $\mathcal{G}$ in the (V,C)-plane (see Figure 1). The analysis of these two points (of which only $P_{-\infty}$ played a role in [12]) is carried out in the next section and shows that in the variables (V,Z), $Z := C^{-2}$, $P_{\pm\infty}$ are saddle points. There are therefore unique trajectories of (1.17) tending to $P_{\pm\infty}$ along which $V \uparrow V_*$. It follows from the uniqueness of these two solutions and from the symmetry properties (1.16) that if $C = C_*(V)$ denotes the solution approaching $P_{+\infty}$, then the solution approaching $P_{-\infty}$ is given as $-C_*(V)$. These trajectories will provide parts of the sought-for similarity solution $(V(x), C(x))$ of (1.11)–(1.12). We therefore have, by construction, that

$$\lim_{x\to\mp\infty}(V(x),C(x)) = P_{\pm\infty}, \tag{3.3}$$

and this ensures that requirement (A) is met.

The requirements (C) and (D), together with the form of (1.11)–(1.12), imply that any relevant solution $(V(x), C(x))$ of these must pass through the origin $(V,C)=(0,0)$ with $x=0$. Thus, the solution we seek must necessarily cross the critical line L_+ on its way from $P_{+\infty}$ to the origin. As the resulting flow we seek is to be continuous for negatives times (corresponding to $x<0$), it follows from (1.11)–(1.12) that the crossing must occur at a critical point of the ODE (1.17).

By exploiting the analysis in [12], we shall show that for each similarity exponent $\lambda \in (1,\hat{\lambda})$ ($\hat{\lambda}$ as in the Main Result and to be determined in the construction process) the unique trajectory of (1.17) approaching $P_{+\infty}$ will connect to a certain critical point $P_8 = (V_8, C_8)$ (notation as in [12]) which is located on the critical line L_+. This solution is given by the function $C_*(V)$; we denote its trajectory by Γ_1, and we shall verify that this is contained in the strip $V_8 < V < V_*$. Also, within this strip, Γ_1 is located below $\mathcal{G}$ and above $\mathcal{F}$, which in turn is located above L_+ (see Figure 1). We are free to choose an x-parametrization of Γ_1 by setting, e.g., $(V(x_0), C(x_0)) := P_8$ for any choice of $x_0 < 0$. This fixes the x-parametrization of the entire solution $(V(x), C(x))$ under consideration.

It turns out that P_8 is a node for (1.17) when $\lambda \in (1,\hat{\lambda})$. There are therefore two ways for the solution to pass through P_8 as x increases through x_0: either smoothly or by changing direction discontinuously at P_8. In the former case an inspection of the phase portrait of (1.17) shows that there are infinitely many trajectories continuing on to the origin after vertically crossing $\mathcal{G}$; we denote any one of these by Γ_2 (see Figure 1). In the latter case there is a unique trajectory denoted Γ_2' connecting P_8 to the

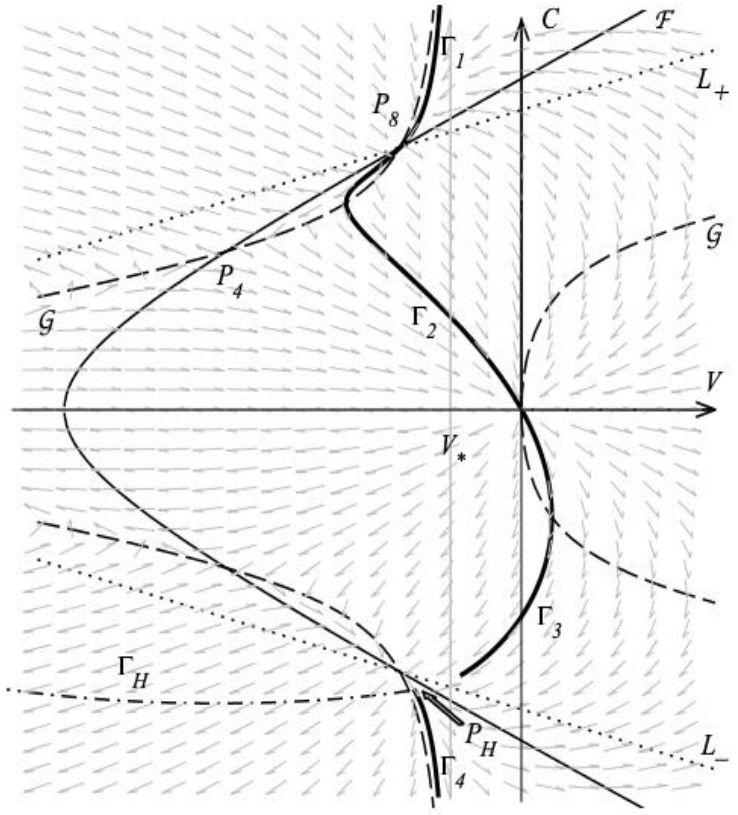

FIG. 1. *A Maple plot of a complete solution of ODE* (1.17) *with* $n = 3$, $\gamma = 3$, $\lambda = 1.22$. *The thick solid curve is the solution consisting of the four parts* Γ_1–Γ_4; *The thin solid curve and the dashed curves are the zero levels* $\mathcal{F}$ *and* $\mathcal{G}$ *of* F *and* G, *respectively; the dotted lines are the critical lines* $L_\pm$; *the gray line is* $V = V_*$ *(the vertical asymptote of* $\mathcal{G}$*); and the dash-dot curve in the lower half-plane is the Hugoniot curve corresponding to* Γ_3. *Note that* Γ_3 *in this case crosses the negative* C*-axis: The corresponding flow undergoes stagnation (vanishing velocity) along a curve* $x = const.$ *located on the outside of the expanding shock.*

origin. In this case the resulting flow will suffer a weak discontinuity (i.e., a gradient discontinuity) across the path $r = (\frac{t}{x_0})^{\frac{1}{\lambda}}$ for $t < 0$, which is a 1-characteristic.

Next, linearizing (1.17) at $(V, C) = (0, 0)$ shows that this is a star point for all choices of n, γ, λ. It follows from (1.11)–(1.12) that any solution $(V(x), C(x))$ approaching the origin does so with both $V(x)$ and $C(x)$ proportional to x, say, $V(x) \sim \nu x$ and $C(x) \sim \mu x$ for $x \lesssim 0$. Thus, there are infinitely many choices for trajectories connecting P_8 to the origin, arriving there with constant slopes $\frac{\mu}{\nu}$. The only constraint is that $\mu \neq 0$; otherwise, according to (1.8), we would have $\rho(0, r) \equiv 0$, which is clearly unphysical.

At this stage, by translating back to ρ and u via (1.8), we have obtained a continuous solution of the radial Euler system (1.6)–(1.7) which suffers blowup of density and velocity at $r = 0$ as $t \uparrow 0$; the blowup profiles are recorded in (4.17)–(4.18) below. To continue to positive times, we need to trace the solution $(V(x), C(x))$ through the origin and into the lower half of the (V, C)-plane. We note that condition (C) requires that the crossing of the origin occurs in a smooth manner.

After passing smoothly through the origin along one of the trajectories Γ_2 (or the particular trajectory Γ_2'), we must next determine the x-value $x_{\rm s} > 0$ at which the solution is to suffer a jump discontinuity. For this, let Γ_3 denote the trajectory of that part of the solution $x \mapsto (V(x), C(x))$ which corresponds to $0 < x < x_{\rm s}$, where $x_{\rm s}$ is to be determined. With x increasing from 0, we apply Lemma 2.1 with $(V(x), C(x))$ for (V_+, C_+) and x for $\bar{x}$ to obtain a unique point $(V_H(x), C_H(x)) = (V_-, C_-)$ with the property that it connects to $(V(x), C(x))$ through an admissible 2-shock. We denote the curve $x \mapsto (V_H(x), C_H(x))$ by Γ_H and refer to it as the "Hugoniot curve" corresponding to Γ_3 (see Figure 1).

Next, let Γ_4 denote the unique trajectory of (1.17) which approaches $P_{-\infty}$; according to the discussion above, this is the graph of the function $-C_*(V)$. To determine $x_{\rm s}$, we need to impose property (Π): Γ_4 must intersect the Hugoniot curve Γ_H at a point $P_H = (V_H(x_{\rm s}), C_H(x_{\rm s}))$ located below L_-. As it turns out, it appears that for Γ_H and Γ_4 to meet, it is necessary that the solution under consideration crosses the origin into the *fourth* quadrant (equivalently, Γ_2 or Γ_2' reach the origin with a finite, *negative* slope). As noted in Remark 1.1 (see Remark 4.7 below for further details), numerical computations indicate that for fixed $n = 2$ or 3, $\gamma > 1$, and $\lambda \in (1, \hat{\lambda}(n, \gamma))$, property ($\Pi$) is satisfied for infinitely many solutions. The property $P_H = (V_H(x_{\rm s}), C_H(x_{\rm s})) \in \Gamma_4$ yields, by definition, the value of $x_{\rm s} > 0$. (Numerics indicate that $\Gamma_4 \cap \Gamma_H$, if nonempty, always consists of a single point; however, this is not essential for our purposes.)

Finally, from $P_H \in \Gamma_4$, the solution follows Γ_4 down to $P_{-\infty} = (V_*, -\infty)$ as $x \to +\infty$, completing the construction of the similarity solution we seek. We note that the solution crosses the critical line L_- by jumping from $(V(x_{\rm s}), C(x_{\rm s}))$ (located strictly above L_-) to P_H (located strictly below L_-) through an admissible 2-shock. In contrast, the solution crossed the critical line L_+ by passing through it at the critical point P_8.

The requirements (A), (C), and (D) will follow from the construction of the solution; the requirements (B) and (E) will be verified separately in sections 4.5 and 4.6, respectively.

We end this section with two points that require further comment, both having to do with the fact that we build solutions of the similarity ODEs (1.11)–(1.12) by first solving the x-independent ODE (1.17) for $C(V)$.

Remark 3.1 (x-parametrization of solutions). As indicated above, we have some freedom in choosing the x-parametrization of solutions to (1.11)–(1.12). For concreteness, consider the solution $C = C_*(V)$, $V_8 \le V < V_*$, of (1.17) whose graph Γ_1 in the (V, C)-plane connects P_8 to $P_{+\infty}$. To obtain a corresponding solution of (1.11)–(1.12), we fix any strictly negative value x_0 and pose the Cauchy problem

$$V'(x) = -\frac{1}{\lambda x}\frac{G(V(x), C_*(V(x)), \lambda)}{D(V(x), C_*(V(x)))}, \tag{3.4}$$

$$V(x_0) = V_8. \tag{3.5}$$

We need to argue that (3.4)–(3.5) has a solution $V(x)$ which is defined for all $x \le x_0$ and that $V(x) \uparrow V_*$ corresponds to $x \downarrow -\infty$. If so, it is immediate to verify that the pair $(V(x), C(x))$, where $C(x) := C_*(V(x))$, solves (1.11)–(1.12) with $(V(x_0), C(x_0)) = P_8$.

The first thing to verify is that the right-hand side of (3.4) remains bounded as $x \uparrow x_0$—which is not obvious since both its numerator and denominator vanish at x_0. As x_0 is chosen strictly negative, the prefactor $-\frac{1}{\lambda x}$ is harmless. For the quotient $\frac{G}{D}$, we make use of the results of section 4 below. Taylor expanding G and D about P_8,

we obtain that for $(V, C) \in \Gamma_1$ near P_8

$$\frac{G(V,C,\lambda)}{D(V,C)} \sim \frac{G_V(V-V_8)+G_C(C-C_8)}{D_V(V-V_8)+D_C(C-C_8)} \sim \frac{G_V+\sigma G_C}{D_V+\sigma D_C},$$

where the partials of G and D are evaluated at P_8 and $\sigma := C_*'(V_8)$. According to Lemma 4.6, $\sigma = \frac{\lambda_- - G_V}{G_C}$, where λ_- is given by (4.16). Thus,

$$\frac{G(V,C,\lambda)}{D(V,C)} \sim \frac{\lambda_-}{D_V+\sigma D_C} = \frac{\lambda_-}{2(1+V_8)(1-\sigma)}.$$

It is readily verified that $\sigma > 1$ in all cases under consideration in section 4 (see Lemma 4.3), and it follows that $\frac{G(V,C,\lambda)}{D(V,C)}$ remains bounded along Γ_1 as $V \downarrow V_8$. This shows that (3.4)–(3.5) is a well-posed initial value problem.

Next, consider the situation as x decreases from x_0; $V(x)$ then increases toward V_*, and we claim that $x \downarrow -\infty$ as $V(x) \uparrow V_*$. Now, as $V(x) \uparrow V_*$, we have $C(x) = C_*(V(x)) \uparrow \infty$, and it follows from the proof of Lemma 4.4 that

$$V'(x) \sim -\frac{2}{\lambda x}(V(x)-V_*) \qquad \text{for } V(x) \text{ near } V_*,$$

which yields the claim. We note that the foregoing arguments also show that if we were to "start" the Cauchy problem for (3.4) at some value $x_1 < x_0$, then P_8 will be reached for a finite x-value.

Finally, similar considerations apply at the origin and at $P_{-\infty}$. Specifically, having started at P_8 with a strictly negative x-value, the solutions under consideration will necessarily pass through the origin for $x = 0$ and tend to $P_{-\infty}$ as $x \uparrow \infty$.

Remark 3.2 (direction of flow). We also need to check that the resulting trajectory $x \mapsto (V(x), C(x))$ moves in the "correct manner" in the (V, C)-plane as x increases from $-\infty$ to $+\infty$. (Along Γ_1, the vector $(V'(x), C'(x))$ given by (1.11)–(1.12) should point in a south-west direction, etc.) This is easily verified once the results of the analysis in section 4 have been obtained. In particular, the verification exploits the fact that the solutions under consideration of the similarity ODEs (1.11)–(1.12) pass through the origin for $x = 0$. For convenience, we have included, for a representative case, the direction field of the similarity ODEs (1.11)–(1.12) in Figure 1.

4. Construction of converging-diverging flows: Details. We next turn to the details of the steps in the outline in section 3. In the process, we impose several constraints on the similarity exponent λ, leading to the definition of $\hat{\lambda} = \hat{\lambda}(n, \gamma)$ in (4.8) below. Note that λ is always assumed to be strictly larger than unity. In the following, we often suppress dependencies on n and γ.

4.1. Critical points of (1.17). The critical points of (1.17) are the points of intersection between the zero level sets $\mathcal{F}$ and $\mathcal{G}$ of F and G, respectively. The location of these depend on λ (as well as n and γ). In section 3 of [12] it was demonstrated that the ODE (1.17) has up to nine critical points in the (V, C)-plane (excluding the critical points $P_{\pm\infty}$ at infinity). We shall follow the terminology and numbering in [12] and denote these by $P_i = (V_i, C_i)$, $i = 1, \ldots, 9$. Due to the properties (1.16), the critical points are located symmetrically about the V-axis. Only four critical points are directly relevant for us: P_4, P_6, P_8, located in the upper half-plane, and $P_1 = (0, 0)$. The locations of the first three points depend on λ, with P_6 and P_8

disappearing for sufficiently large values of λ. For our purposes, we shall need that P_6 and P_8 exist and satisfy $V_6 < V_4 < V_8$.

First, recall that $\mathcal{G}$ has a vertical asymptote located at $V = V_* = \frac{\kappa}{n} < 0$. The analysis in [12] establishes that, with

(4.1)
$$z = z(\lambda) := \tfrac{\lambda-1}{(n-1)(\gamma-1)} \qquad \text{and} \qquad w = w(z) := +\sqrt{(\gamma-3)^2 z^2 - 2(\gamma+1)z + 1},$$

the values of V_4, V_6, and V_8 are given by

$$V_4 = -\tfrac{\lambda}{1+\frac{n}{2}(\gamma-1)}, \qquad V_6 = \tfrac{1}{2}[-w + (\gamma-3)z - 1], \qquad V_8 = \tfrac{1}{2}[w + (\gamma-3)z - 1]. \tag{4.2}$$

We want our solutions to pass through P_8, which requires that w is a real number. This gives the first condition on λ: A calculation shows that w is real and strictly positive provided

$$1 < \lambda < \lambda_{\max} := 1 + \tfrac{(n-1)(\gamma-1)}{(\sqrt{\gamma-1}+\sqrt{2})^2}, \tag{4.3}$$

which is assumed from now on, in particular, $V_6 < V_8$. A direct calculation verifies the nonobvious fact that both P_6 and P_8 lie on the critical line L_+ (cf. (3.1)).

LEMMA 4.1. *Assuming that $n = 2$ or 3 and $\gamma > 1$ and that (4.3) is satisfied, we have*

$$-1 < V_4,\, V_6,\, V_8 < V_* < 0. \tag{4.4}$$

Proof. With one exception, these inequalities are straightforward to verify by using the expressions in (4.2). For example, a calculation shows that $-1 < V_4 < V_*$ holds if and only if $\lambda < 1 + \frac{n}{2}(\gamma-1)$, which is easily seen to hold when (4.3) is met. Only the inequality $V_8 < V_*$ requires more work. It may be rewritten as

$$w < 1 - \tfrac{4(\lambda-1)}{n(\gamma-1)} - (\gamma-3)z. \tag{4.5}$$

A calculation shows that the right-hand side of (4.5) is positive provided $\lambda < 1 + \frac{n(n-1)(\gamma-1)}{n(\gamma+1)-4}$, which is indeed the case when (4.3) holds. Thus, by squaring both sides of (4.5), substituting from (4.1), and simplifying, we obtain that $V_8 < V_*$ if and only if

$$0 < (\gamma-1) + (\lambda-1)[(\gamma-1) - \tfrac{2}{n}].$$

This is clearly satisfied if $\gamma - 1 \geq \frac{2}{n}$; in the opposite case, we rewrite the last inequality as

$$\lambda < 1 + \tfrac{n(\gamma-1)}{2-n(\gamma-1)},$$

which turns out to hold whenever (4.3) is met. ∎

LEMMA 4.2. *Assuming $n = 2$ or 3 and $\gamma > 1$, there is a $\tilde{\lambda} = \tilde{\lambda}(\gamma, n) > 1$ so that*

$$V_6 < V_4 < V_8 \qquad \textit{whenever } 1 < \lambda < \tilde{\lambda}. \tag{4.6}$$

Proof. Define $g(\lambda) := V_8(\lambda) - V_4(\lambda)$ and $h(\lambda) := V_4(\lambda) - V_6(\lambda)$. Direct calculations using the expressions in (4.1) yield $g(1)$, $h(1) > 0$, $g'(1)$, $h'(1) < 0$, and $g''(\lambda)$, $h''(\lambda) < 0$. It follows that both $g(\lambda)$ and $h(\lambda)$ are strictly decreasing on $[1, \lambda_{\max}]$. If g remains positive on this interval, we set $\lambda_g := \lambda_{\max}$; otherwise, we let λ_g denote the unique zero of g. We similarly define λ_h. Finally, setting $\tilde{\lambda} := \min(\lambda_g, \lambda_h)$, we obtain the claim. ∎

We shall require that the resulting radial flow has locally finite energy, and this will impose an additional constraint on the possible values of the similarity exponent:

$$1 < \lambda < \bar{\lambda} := 1 + \tfrac{n}{2}(1 - \tfrac{1}{\gamma}); \tag{4.7}$$

see the proof of Proposition 4.8 below. We now define

$$\hat{\lambda} = \hat{\lambda}(\gamma, n) := \min(\tilde{\lambda}, \bar{\lambda}). \tag{4.8}$$

This is the $\hat{\lambda}$ in the Main Result, and the restriction

$$1 < \lambda < \hat{\lambda} \tag{4.9}$$

is assumed from here on.

4.2. The trajectory Γ_1. We next show that there is a unique trajectory of (1.17), denoted Γ_1, connecting $P_{-\infty} = (V_*, +\infty)$ to P_8. We first analyze the relative locations of $\mathcal{F}$, $\mathcal{G}$, L_+.

LEMMA 4.3. *Assume* (4.9) *holds. Then, within the half-strip* $\mathbb{S} := \{(V, C) \,|\, V_8 < V < V_*, C > 0\}$, *we have the situation depicted in Figure* 1: $\mathcal{G}$ *is located above* $\mathcal{F}$, *and* $\mathcal{F}$ *is located above* L_+ *in the* (V, C)*-plane.*

Proof. It follows from the results above and the analysis in [12] that there is no point of intersection between $\mathcal{F}$ and $\mathcal{G}$ within $\mathbb{S}$. Since $C \uparrow +\infty$ along $\mathcal{G}$ and C remains finite along $\mathcal{F}$, as $V \uparrow V_*$, it follows that $\mathcal{G}$ lies above $\mathcal{F}$ within $\mathbb{S}$. Next, according to (1.15), we have that $\mathcal{F}$ within $\mathbb{S}$ is the graph of $C_F(V) := +\sqrt{k_1(1+V)^2 - k_2(1+V) + k_3}$. Thus, $\mathcal{F}$ lies above L_+ there provided

$$C_F(V) > 1 + V \qquad \text{for } V_8 < V < V_*, \tag{4.10}$$

or, equivalently,

$$f(V) := (k_1 - 1)(1+V)^2 - k_2(1+V) + k_3 > 0 \qquad \text{for } V_8 < V < V_*. \tag{4.11}$$

Since $P_8 \in \mathcal{F} \cap L_+$, $f(V_8) = 0$. As $f(V)$ is quadratic in V with a positive leading coefficient, (4.11) follows once we verify that $f'(V_8) > 0$. A calculation using (4.2) and $(4.1)_1$ shows that $f'(V_8) > 0$ if and only if $w(z(\lambda)) > 0$, which is satisfied for all $\lambda \in (1, \hat{\lambda})$. ∎

LEMMA 4.4. *Assume* (4.9) *holds. Then there is a unique solution* $C = C_*(V)$ *of the ODE* (1.17) *passing through* P_8 *and satisfying* $C_*(V) \uparrow +\infty$ *as* $V \uparrow V_*$. *Its trajectory* Γ_1 *is located below* $\mathcal{G}$ *and above* $\mathcal{F}$ *(see Figure* 1*).*

Proof. By changing variables to $W := V - V_*$ and $Z := C^{-2}$ and linearizing the ODE for dZ/dW at $(W, Z) = (0, 0)$, we obtain

$$\frac{dZ}{dW} = -\frac{2Z}{nW - \alpha Z}, \qquad \text{where } \alpha = (1 + V_*)V_*(\lambda + V_*) < 0. \tag{4.12}$$

It follows that the origin in the (W, Z)-plane is a hyperbolic rest point for (4.12), that the latter has a unique solution $Z_*(W)$ passing through the origin, and that $Z_*(W)$ approaches the origin along the straight line $Z = \frac{n+2}{\alpha}W$, which has negative slope in the (W, Z)-plane. Translating back to (V, C)-variables, we conclude that there is a unique solution $C_*(V) := (Z_*(V - V_*))^{-\frac{1}{2}}$ of (1.17) satisfying $C_*(V) \uparrow +\infty$ as $V \uparrow V_*$. Finally, consider any solution $C(V)$ of (1.17) passing through any point in $\mathbb{S}$ located in the region between $\mathcal{F}$ and $\mathcal{G}$. It follows from the signs of F and G there that the solution cannot exit this region as $V \downarrow V_8$, and it must therefore approach C_8 as $V \downarrow V_8$. In particular, this applies to the solution $C_*(V)$. ∎

We next analyze the critical point P_8, whose type depends on the eigenvalues of the matrix

$$A_8 = \begin{bmatrix} G_V & G_C \\ F_V & F_C \end{bmatrix},$$

where the partials derivatives are evaluated at (V_8, C_8, λ). To determine the signs and relative sizes of these, we first note that the Wronskian $\mathcal{W}_8 = G_V F_C - G_C F_V$ at P_8 is given by

$$\mathcal{W}_8 = 2kC_8^2(V_8 - V_4)(V_8 - V_6) \qquad \text{for a constant } k > 0$$

(see equation $(5.11)_3$ in [12]). According to Lemma 4.2 and the standing assumption (4.9), we thus have $\mathcal{W}_8 > 0$ for all λ under consideration.

LEMMA 4.5. *Assume* (4.9) *holds. Then, at* P_8*, we have*

$$F_C > 0, \quad G_C < 0, \quad G_V + G_C > 0, \quad F_V + F_C < 0. \tag{4.13}$$

It follows that $F_V < 0$*,* $G_V > 0$*, and* $G_V + F_C > 0$ *at* P_8*.*

Proof. Throughout, all partials are evaluated at P_8. By using that P_8 is a zero of F, G, and $1 - V - C$, we obtain $F_C = 2C^2 > 0$ and $G_C = 2V(\lambda + V) < 0$. A similar calculation shows that $G_V + G_C = (n-1)Cw > 0$. It follows that $G_V > 0$, and hence $G_V + F_C > 0$. Finally, by differentiating the identity $F(V, 1+V, \lambda) \equiv -\frac{\gamma-1}{2}G(V, 1+V, \lambda)$ with respect to V, we obtain $F_V + F_C = -\frac{\gamma-1}{2}(G_V + G_C) < 0$, and thus $F_V < -F_C < 0$. ∎

LEMMA 4.6. *Assume* (4.9) *holds. Then the matrix* A_8 *has two real and strictly positive eigenvalues* $0 < \lambda_- < \lambda_+$*. The corresponding eigenvectors* $r_\pm$ *are parallel to lines with slopes*

$$\frac{\lambda_\pm - G_V}{G_C} = \frac{(F_C - G_V) \pm \sqrt{(F_C - G_V)^2 + 4G_C F_V}}{2G_C}, \tag{4.14}$$

respectively, and these slopes satisfy

$$\frac{\lambda_+ - G_V}{G_C} < 0 < \frac{\lambda_- - G_V}{G_C}. \tag{4.15}$$

Proof. The eigenvalues $\lambda_\pm$ of A_8 are given by

$$\lambda_\pm = \frac{(G_V + F_C) \pm \sqrt{(G_V + F_C)^2 - 4\mathcal{W}_8}}{2} \equiv \frac{(G_V + F_C) \pm \sqrt{(G_V - F_C)^2 + 4G_C F_V}}{2}. \tag{4.16}$$

Lemma 4.5 gives $G_C F_V > 0$, so that the radicand in (4.16) is positive and $\lambda_\pm$ are real. As $\mathcal{W}_8 > 0$, the first expression gives $\operatorname{sgn} \lambda_\pm = \operatorname{sgn}(G_V + F_C)$, which, by Lemma 4.5, is positive. Therefore, $0 < \lambda_- < \lambda_+$. A direct calculation shows that the corresponding eigenvectors $r_\pm$ are parallel to lines with slopes given by (4.14). Again by Lemma 4.5, $G_C F_V > 0 > G_C$, giving (4.15). ∎

It follows from Lemmas 4.4 and 4.6 that the unique solution $C_*(V)$ of (1.17) introduced above approaches P_8 with positive slope along r_-. We now choose any $x_0 < 0$ and fix the parametrization of the solution $(V(x), C(x))$ under construction by requiring that $(V(x_0), C(x_0)) = P_8$.

4.3. The trajectories Γ_2 and Γ_2'. Assuming (4.9), Lemma 4.6 shows that P_8 is a node. Thus, there are two ways to continue the solution $(V(x), C(x))$ from P_8 (see section 3): either in the same direction as $C_*(V)$ reached P_8 (i.e., parallel to r_-) or by changing direction and leaving P_8 with increasing $V(x)$ and decreasing $C(x)$ in the direction parallel to r_+. In the former case, both $V(x)$ and $C(x)$ will start out decreasing. In this case there are infinitely many continuations to choose from, the only requirement being that the trajectory crosses the zero level $\mathcal{G}$ before continuing on to the origin in the (V, C)-plane (see Figure 1). For all such solutions the resulting flow will be smooth. If instead we choose to leave P_8 parallel to r_+ (with V increasing and C decreasing), the flow will suffer a "kink"; i.e., the first partials of ρ and u will be discontinuous across the curve $r_0(t) := (\frac{t}{x_0})^{\frac{1}{\lambda}}$. A gradient discontinuity in an otherwise smooth flow can propagate only along a characteristic curve [5], and this is the case here: Since $P_8 \in L_+$, we have $C(x_0) - V(x_0) = 1$, which gives $\dot{r_0}(t) = u(t, r_0(t)) - c(t, r_0(t))$; i.e., $r_0(t)$ is a 1-characteristic.

Next, the linearization of (1.17) at $P_1 = (0, 0)$ is $\frac{dC}{dV} = \frac{(-k_1+k_2-k_3)C}{(-\lambda)V} = \frac{C}{V}$, so that the origin is a star point. Linearizing (1.11) and (1.12) at the origin, we obtain $\frac{dV}{V}$, $\frac{dC}{C} \sim \frac{dx}{x}$. It follows that both $V(x)$ and $C(x)$ approach the origin proportionally to x: $V(x) \sim \nu x$ and $C(x) \sim \mu x$ for $x \lesssim 0$, where μ and ν are constants. The ratio $\frac{\mu}{\nu}$ is the slope with which the chosen trajectory from P_8 reaches the star point P_1. This slope parametrizes the solutions through the origin, and since there are infinitely many trajectories of (1.17) that connect P_8 to it, it follows that there are infinitely many trajectories through P_8 that reach the origin. As noted in section 3, the only restriction in choosing one of the trajectories Γ_2 (or Γ_2') is that $\mu = \lim_{x\to 0} \frac{C(x)}{x}$ must be strictly negative (to avoid an everywhere vanishing density field at time $t = 0$).

We note that both P_8 and P_1 are critical points of (1.17) and that we have a choice as to how the solution passes through P_8. However, no such choice is available for P_1: Condition (C) requires in particular that the two limits $\lim_{x\to 0\pm} \frac{C(x)}{V(x)}$ agree. Therefore, the solution must pass smoothly through the origin; as the latter is a star point, this determines uniquely the continuation of Γ_2 (or Γ_2') into the lower half-plane.

Finally, let us express explicitly the flow variables at time $t = 0$. With the notation introduced above, (1.8) gives

$$u(0, r) = -\tfrac{\nu}{\lambda} r^{1-\lambda}, \qquad c(0, r) = -\tfrac{\mu}{\lambda} r^{1-\lambda} \tag{4.17}$$

and

$$\rho(0, r) = K r^{\kappa}, \qquad K = \left[\tfrac{\mu^2}{\gamma\lambda^2 a^2}\right]^{\frac{1}{\gamma-1}}, \ \kappa = -\tfrac{2(\lambda-1)}{\gamma-1}. \tag{4.18}$$

Since $\lambda > 1$, this shows that u, c, ρ and thus also p all blow up at the origin at time $t = 0$. This establishes part (1) of the Main Result.

4.4. The trajectories Γ_3 and Γ_4 and property (Π). We next trace the chosen solution $(V(x), C(x))$ through the origin and into the lower half-plane for $x > 0$. The trajectory of (1.17) corresponding to $0 < x < x_s$ is denoted Γ_3. Here, x_s is to be determined so that it gives the path $r_s(t) = (\frac{t}{x_s})^{\frac{1}{\lambda}}$ of an admissible 2-shock in the (r, t)-plane, connecting Γ_3 to the unique trajectory Γ_4 of (1.17), which approaches the critical point $P_{+\infty} = (V_*, -\infty)$. As noted earlier, Γ_4 is the graph of $-C_*(V)$, $C_*(V)$ being the unique trajectory approaching $P_{+\infty} = (V_*, +\infty)$.

Since Γ_3 starts out from the origin, it follows that there is an $x' > 0$ so that $(V(x), C(x))$ is located strictly above L_- for $x \in (0, x')$. For each such x, we ap-

ply Lemma 2.1 with $(V_+, C_+) = (V(x), C(x))$ and $\bar{x} = x$ to obtain a unique point $(V_-, C_-) \equiv (V_H(x), C_H(x))$ with the property that the latter point is the inside state of an admissible 2-shock with outside state $(V(x), C(x))$. We denote the curve $x \mapsto (V_H(x), C_H(x))$ by Γ_H and refer to it as the Hugoniot curve corresponding to Γ_3. It follows from Lemma 2.1 that $(V_H(x), C_H(x))$ is located strictly below L_- for each $x \in (0, x')$. The defining property of x_s is that the trajectory starting from the point $(V_H(x_s), C_H(x_s))$ is part of the trajectory Γ_4, i.e., x_s is defined by the requirement that

$$-C_*(V_H(x_s)) = C_H(x_s).$$

As discussed earlier, we have found it necessary to assume that this equation has a solution:

(Π) The trajectory Γ_4 intersects the Hugoniot curve Γ_H corresponding to Γ_3 at a point below the critical line L_-.

If Γ_4 were to intersect Γ_H in more than one point (located below L_-), any one of these will work for our purposes.

Remark 4.7. As noted above, numerical calculations indicate that for fixed $n = 2$ or 3, $\gamma > 1$, and $\lambda \in (1, \hat{\lambda}(n, \gamma))$, there are infinitely many solutions of (1.17) satisfying property (Π). On the other hand, it appears that for fixed $n = 2$ or 3 and $\gamma > 1$ and λ sufficiently small, there are choices of Γ_2 or Γ_2' that generate solutions violating (Π). Based on the numerical evidence we have analyzed, we conjecture that property (Π) is satisfied if and only if Γ_2 or Γ_2' arrives at the origin with a finite and strictly negative slope. This is reasonable on physical grounds: Assuming $\mu < 0$, Γ_2 or Γ_2' will reach the origin with a finite and strictly negative slope if and only if $\nu > 0$. According to (4.17), this means that the fluid velocity is everywhere directed inward at time of collapse ($t = 0$), with unbounded amplitude of the velocity as one approaches the origin. It is reasonable to expect that such initial data at $t = 0$ will necessarily generate an expanding shock wave.

In fact, we further conjecture that if the solution $(V(x), C(x))$ arrives at the origin with either a positive or an infinite slope (such that the fluid at $t = 0$ is everywhere either outward moving or at rest, respectively), then the corresponding flow will remain smooth for all times. We shall not pursue such scenarios in this work and instead focus on cases where a shock wave is generated at the center of motion.

Having thus determined x_s, we solve (1.11)–(1.12) for $x \in (x_s, +\infty)$ with initial condition $(V(x_s), C(x_s)) = (V_H(x_s), C_H(x_s))$. By construction the solution therefore approaches $P_{-\infty} = (V_*, -\infty)$ as $x \uparrow +\infty$. This concludes the construction of the relevant solution $(V(x), C(x))$ of (1.11)–(1.12), which finally yields (via (1.8)) the globally defined similarity solutions $(\rho(t, r), u(t, r))$ described in the Main Result.

Note that the requirements (A) and (C) are satisfied by construction. The same applies to requirement (D): The solutions cross from the upper to the lower half of the (V, C)-plane by passing through the origin for $x = 0$, and they do so with $\lim_{x\to 0} \frac{C(x)}{x} = \mu < 0$. This shows that $\frac{C(x)}{x} < 0$ for all $x \in \mathbb{R}$, verifying requirement (D). Requirements (B) and (E) are verified in the following two subsections. Finally, the analysis in section 5 will verify that the constructed solutions provide weak solutions to the original, multi-d Euler system (1.1)–(1.2).

4.5. Behavior at $x = \pm\infty$. By (3.3) the solutions $(V(x), C(x))$ under consideration satisfy

$$V(x) \uparrow V_* \qquad \text{and} \qquad C(x) \to \pm\infty \qquad \text{as } x \to \mp\infty.$$

In order to analyze the local energy content of the solutions and also the weak forms of the equations, we shall need the leading order behavior of $C(x)$ as $x \to \pm\infty$. Consider the case $x \downarrow -\infty$. We follow [12] and posit series expansions of the forms

$$V(x) = V_* + V_1 y + V_2 y^2 + \cdots \qquad \text{and} \qquad C(x) = y^{-1} + C_0 + C_1 y + \cdots, \tag{4.19}$$

where $y := k|x|^{-\sigma}$ for positive constants k, σ. To determine the exponent σ, we write the ODE (1.12) in terms of y in the form

$$\lambda\sigma y C'(y) D(V(y), C(y)) = F(V(y), C(y), \lambda),$$

substitute from (4.19), and collect powers of y. We obtain $\lambda\sigma y^{-3} + \cdots = y^{-3} + \cdots$, giving $\sigma = \frac{1}{\lambda}$. A similar calculation applies as $x \uparrow +\infty$, and we conclude that

$$V(x) \sim V_* \qquad \text{and} \qquad |C(x)| \sim |x|^{\frac{1}{\lambda}} \qquad \text{as } x \to \pm\infty. \tag{4.20}$$

Specifically, this shows that requirement (B) is satisfied by the solutions under consideration.

4.6. Time continuity and locally bounded total energy. It remains to verify requirement (E), i.e., locally bounded total energy, for the solutions constructed above. It is convenient to establish this as a consequence of a more general continuity result which will be used to show that the solutions in question are genuine weak solutions of the multi-d Euler system (1.1)–(1.2) (see section 5).

PROPOSITION 4.8. *Consider the radial isentropic Euler system* (1.3)–(1.4) *and* (1.5) *in dimension* $n = 2$ *or* 3. *Assume that the similarity exponent* λ *satisfies* (4.9), *and let* ρ, u *be given by* (1.8), *where* (V, C) *is the solution of* (1.11)–(1.12) *constructed in sections* 4.1–4.4. *Then the maps* $t \mapsto \rho(t)^q$ *for* $q \in [1, \gamma]$ *and* $t \mapsto \rho(t)u(t)^k$ *for* $k = 1, 2$ *are continuous as maps from* $\mathbb{R}_t$ *into* $L^1_{loc}(\mathbb{R}^+; r^m dr)$.

Proof. The argument is similar for both types of maps, and we give the details for the representative case $t \mapsto \rho(t)u(t)^k$, $(k = 1, 2)$. We first argue that $\rho(t)u(t)^k$ belongs to $L^1_{loc}(\mathbb{R}^+; r^m dr)$ at all times $t \in \mathbb{R}$. Fix $\bar{r} > 0$. For $t \neq 0$, (1.8) and (1.10) give

$$\|\rho(t)u(t)^k\|_{L^1((0,\bar{r});r^m dr)} \sim \int_0^{\bar{r}} r^{\kappa+m+k(1-\lambda)} \left|\frac{C(t/r^\lambda)}{t/r^\lambda}\right|^{\frac{2}{\gamma-1}} \left|\frac{V(t/r^\lambda)}{t/r^\lambda}\right|^k dr. \tag{4.21}$$

According to the construction of $V(x)$ and $C(x)$ above, $V(x)$ is globally bounded, while $\frac{|C(x)|}{|x|}$ remains bounded as $x \to 0$. In particular, $(4.20)_2$ implies that

$$\left|\frac{C(x)}{x}\right| \lesssim x^{\frac{1}{\lambda}-1} \qquad \text{for } x \in (0, \infty). \tag{4.22}$$

Using this in (4.21) gives

$$\|\rho(t)u(t)^k\|_{L^1((0,\bar{r});r^m dr)} \lesssim |t|^{\frac{\kappa}{\lambda}-k} \int_0^{\bar{r}} r^{m+k}\, dr < \infty \qquad \text{for } t \neq 0.$$

For $t = 0$, (4.18) and (4.17) give

$$\|\rho(0)u(0)^k\|_{L^1((0,\bar{r});r^m dr)} \sim \int_0^{\bar{r}} r^{\kappa+m+k(1-\lambda)}\, dr.$$

The last integral is finite provided $\kappa + m + k(1-\lambda) > -1$, or, equivalently, $\lambda < 1 + \frac{n(\gamma-1)}{k(\gamma-1)+2}$. The stricter constraint occurs for $k = 2$, which requires that $\lambda < \bar{\lambda}$ (see (4.7)), which holds by assumption since $\hat{\lambda} \le \bar{\lambda}$. This shows that $\rho(t)u(t)^k \in L^1_{loc}(\mathbb{R}^+; r^m dr)$ for $k = 1, 2$ and for all times $t \in \mathbb{R}$.

Next, consider the continuity of $t \mapsto \rho(t)u(t)^k$ at any time $t \neq 0$. For $s \approx t$, with $\operatorname{sgn} s = \operatorname{sgn} t$, we have

$$\begin{aligned}&\|\rho(t)u(t)^k - \rho(s)u(s)^k\|_{L^1((0,\bar{r});r^m dr)}\\ &\quad\sim \int_0^{\bar{r}} r^{\kappa+m+k(1-\lambda)} \left| \left|\tfrac{C(t/r^\lambda)}{t/r^\lambda}\right|^{\frac{2}{\gamma-1}} \left(\tfrac{V(t/r^\lambda)}{t/r^\lambda}\right)^k - \left|\tfrac{C(s/r^\lambda)}{s/r^\lambda}\right|^{\frac{2}{\gamma-1}} \left(\tfrac{V(s/r^\lambda)}{s/r^\lambda}\right)^k \right| dr.\end{aligned}$$

Since $C(x)$ and $V(x)$ are almost everywhere continuous, the integrand tends pointwise a.e. to zero as $s \to t$. To bound the integrand by a fixed $L^1((0,\bar{r}); dr)$-function, we use (4.22) and the boundedness of $V(x)$ to get that the integrand in the last integral is bounded by

$$r^{\kappa+m+k(1-\lambda)} \left(|t|^{\frac{\kappa}{\lambda}-k} r^{\lambda k-\kappa} + |s|^{\frac{\kappa}{\lambda}-k} r^{\lambda k-\kappa} \right) \lesssim r^{m+k} \in L^1((0,\bar{r}); dr).$$

An application of the dominated convergence theorem now shows that $\rho(s)u(s)^k \to \rho(t)u(t)^k$ in $L^1((0,\bar{r}); r^m dr)$ when $s \to t \neq 0$.

However, the last estimate involves a multiplicative factor $\sim |t|^{\frac{\kappa}{\lambda}-k}$, and a more detailed argument is required for $t = 0$. We have from (4.18) and (4.17) that

$$\begin{aligned}&\|\rho(0)u(0)^k - \rho(s)u(s)^k\|_{L^1((0,\bar{r});r^m dr)}\\ &\quad\sim \int_0^{\bar{r}} r^{\kappa+m+k(1-\lambda)} \left| \mu^{\frac{2}{\gamma-1}} \nu^k - \left|\tfrac{C(s/r^\lambda)}{s/r^\lambda}\right|^{\frac{2}{\gamma-1}} \left(\tfrac{V(s/r^\lambda)}{s/r^\lambda}\right)^k \right| dr.\end{aligned} \tag{4.23}$$

Since $\frac{C(x)}{x} \to \mu$ and $\frac{V(x)}{x} \to \nu$ as $x \to 0$, we have that the integrand in (4.23) tends pointwise to zero as $s \to 0$. To uniformly bound the integrand, we observe that the constructed solutions $C(x)$ and $V(x)$ satisfy

$$\left|\tfrac{C(x)}{x}\right|, \left|\tfrac{V(x)}{x}\right| \lesssim 1 \quad \text{for } |x| \le 1, \text{ while } \left|\tfrac{C(x)}{x}\right| \lesssim |x|^{\frac{1}{\lambda}-1}, |V(x)| \lesssim 1 \quad \text{for } |x| \ge 1. \tag{4.24}$$

Using these properties, we get that the integrand in (4.23) is bounded (up to a multiplicative constant) by

$$r^{\kappa+m+k(1-\lambda)} \left(1 + \chi_{[0,|s|^{\frac{1}{\lambda}}]}(r) \left(\tfrac{|s|}{r^\lambda}\right)^{\frac{\kappa}{\lambda}-k}\right) = r^{\kappa+m+k(1-\lambda)} + |s|^{\frac{\kappa}{\lambda}-k} \chi_{[0,|s|^{\frac{1}{\lambda}}]}(r) r^{m+k}.$$

In the last expression, the values of the second term are pointwise bounded by those of the first term (agreeing at $r = |s|^{\frac{1}{\lambda}}$). It follows that the integrand in (4.23) is pointwise bounded by a constant multiple of $r^{\kappa+m+k(1-\lambda)}$. Finally, as shown above, the latter function belongs to $L^1((0,\bar{r}); dr)$ for all λ-values under consideration. The dominated convergence theorem therefore gives that $\rho(s)u(s)^k \to \rho(0)u(0)^k$ in $L^1((0,\bar{r}); r^m dr)$ as $s \to 0$. This establishes the stated continuity of the map $t \mapsto \rho(t)u(t)^k$ for $k = 1, 2$ at all times $t \in \mathbb{R}$. ∎

We recall [6] that the total energy of the radial solution $(\rho, u)(t, r)$ within the ball of radius $\bar{r} > 0$ about the origin is given as

$$E(t,\bar{r}) := \int_0^{\bar{r}} (\tfrac{1}{2}\rho u^2 + \tfrac{a^2}{\gamma-1}\rho^\gamma) r^{n-1}\, dr.$$

Thanks to the continuity of the maps $t \mapsto \rho(t)u(t)^2$, $\rho(t)^\gamma \in L^1_{loc}(\mathbb{R}^+; r^m dr)$, we thus have the following.

COROLLARY 4.9. *With the same setting and assumptions as in Proposition* 4.8, *the radial similarity solutions constructed in sections* 4.1–4.4 *satisfy requirement* (E).

5. Radial similarity solutions as weak solutions to multi-d Euler. In section 5.1, we first give the definition of general weak solutions of the original, multi-d Euler system (1.1)–(1.2) and specialize it to radial solutions. We then verify that the radial similarity solutions generated above satisfy the latter definition, thereby showing that they provide genuine weak solutions of (1.1)–(1.2).

5.1. Weak and radial weak Euler solutions. We write $\rho(t)$ for $\rho(t,\cdot)$ etc., $\mathbf{u} = (u_1, \dots, u_n)$, $u := |\mathbf{u}|$, and let $\mathbf{x} = (x_1, \dots, x_n)$ denote the spatial variable in $\mathbb{R}^n$.

DEFINITION 5.1. *Consider the compressible Euler system* (1.1)–(1.2) *in* n *space dimensions with pressure function* $p = p(\rho)$. *The measurable functions* $\rho, u_1, \dots, u_n : \mathbb{R}_t \times \mathbb{R}^n_{\mathbf{x}} \to \mathbb{R}$ *constitute a* weak solution *of* (1.1)–(1.2) *provided that*

(1) *the maps* $t \mapsto \rho(t)$ *and* $t \mapsto \rho(t)u(t)$ *belong to* $C^0(\mathbb{R}_t; L^1_{loc}(\mathbb{R}^n_{\mathbf{x}}))$;
(2) *the functions* ρu^2 *and* $p(\rho)$ *belong to* $L^1_{loc}(\mathbb{R}_t \times \mathbb{R}^n_{\mathbf{x}})$;
(3) *the conservation laws for mass and momentum are satisfied weakly in sense that*

$$\int_{\mathbb{R}} \int_{\mathbb{R}^n} \rho\varphi_t + \rho\mathbf{u} \cdot \nabla_{\mathbf{x}}\varphi \, d\mathbf{x}dt = 0 \tag{5.1}$$

and

$$\int_{\mathbb{R}} \int_{\mathbb{R}^n} \rho u_i \varphi_t + \rho u_i \mathbf{u} \cdot \nabla_{\mathbf{x}}\varphi + p(\rho)\varphi_{x_i} \, d\mathbf{x}dt = 0 \qquad \text{for } i = 1, \dots, n \tag{5.2}$$

whenever $\varphi \in C^1_c(\mathbb{R}_t \times \mathbb{R}^n_{\mathbf{x}})$ *(the set of* C^1 *functions with compact support).*

Remark 5.2. In this definition, condition (1) requires that the conserved quantities define continuous maps into $L^1_{loc}(\mathbb{R}^n_{\mathbf{x}})$, which is the natural function space in this setting. Taken together, conditions (1) and (2) ensure that all terms occurring in the weak formulations (5.1) and (5.2) are locally integrable in space and time.

We next rewrite Definition 5.1 for radial solutions. For this, we set $r = |\mathbf{x}|$, $m = n - 1$, and

$$\mathbb{R}^+ = (0, \infty), \qquad \mathbb{R}^+_0 = [0, \infty), \qquad L^1_{(loc)}(dt \times r^m dr) = L^1_{(loc)}(\mathbb{R} \times \mathbb{R}^+_0, dt \times r^m dr).$$

It is convenient to introduce the following (nonstandard) notation: $C^1_c(\mathbb{R} \times \mathbb{R}^+_0)$ denotes the set of real-valued C^1 functions $\psi : \mathbb{R} \times \mathbb{R}^+_0 \to \mathbb{R}$ that vanish outside $[-\bar{t}, \bar{t}] \times [0, \bar{r}]$ for some $\bar{t}, \bar{r} \in \mathbb{R}^+$. Also, $C^1_0(\mathbb{R} \times \mathbb{R}^+_0)$ denotes the set of those $\theta \in C^1_c(\mathbb{R} \times \mathbb{R}^+_0)$ with the additional property that $\theta(t, 0) \equiv 0$.

DEFINITION 5.3. *With the same setup as in Definition* 5.1, *the measurable functions* $\rho, u : \mathbb{R}_t \times \mathbb{R}^+_r \to \mathbb{R}$ *constitute a* radial weak solution *of* (1.4)–(1.5) *provided that*

(i) *the maps* $t \mapsto \rho(t)$ *and* $t \mapsto \rho(t)u(t)$ *belong to* $C^0(\mathbb{R}_t; L^1_{loc}(r^m dr))$;
(ii) *the functions* ρu^2 *and* $p(\rho)$ *belong to* $L^1_{loc}(dt \times r^m dr)$;

(iii) *the conservation laws for mass and momentum are satisfied in the sense that*

$$\int_{\mathbb{R}}\int_{\mathbb{R}^+} (\rho\psi_t + \rho u\psi_r)\, r^m dr dt = 0 \qquad \forall \psi \in C_c^1(\mathbb{R}\times\mathbb{R}_0^+), \tag{5.3}$$

$$\int_{\mathbb{R}}\int_{\mathbb{R}^+} \big(\rho u\theta_t + \rho u^2\theta_r + p(\rho)\big(\theta_r + \tfrac{m\theta}{r}\big)\big)\, r^m dr dt = 0 \qquad \forall \theta \in C_0^1(\mathbb{R}\times\mathbb{R}_0^+). \tag{5.4}$$

We record the fact that the latter definition is consistent with the former one as follows.

PROPOSITION 5.4. *Assume that* $(\rho(t,r), u(t,r))$ *is a radial weak solution of* (1.4)–(1.5) *according to Definition* 5.3*, and define the functions*

$$\rho(t,\mathbf{x}) := \rho(t,|\mathbf{x}|), \qquad \mathbf{u}(t,\mathbf{x}) := u(t,|\mathbf{x}|)\frac{\mathbf{x}}{|\mathbf{x}|}. \tag{5.5}$$

Then $(\rho,\mathbf{u})$ *is a weak solution of the multi-d system* (1.1)–(1.2) *according to Definition* 5.1.

Proof. This was established in [9] (Theorem 5.7) for the isothermal Navier–Stokes system; the same proof applies to the Euler system. ∎

5.2. Verification of weak forms of the equations. For fixed parameters n and λ as in the Main Result, we let $\rho(t,r)$ and $u(t,r)$ be the similarity solutions constructed above. It follows from Proposition 4.8 that (ρ,u) satisfies parts (i) and (ii) of Definition 5.3. Thus, to verify that (ρ,u) provides a radial weak solution to the isentropic Euler system, it only remains to argue for part (iii) of Definition 5.3, i.e., the weak forms of the equations.

For this, we fix $\psi \in C_c^1(\mathbb{R}\times\mathbb{R}_0^+)$ and $\theta \in C_0^1(\mathbb{R}\times\mathbb{R}_0^+)$ (recall the definition of these function spaces above) with $\operatorname{supp}\psi$, $\operatorname{supp}\theta \subset [-T,T]\times[0,\bar r]$. As in Definition 5.3, ψ and θ will be test functions for the mass and momentum equations (5.3) and (5.4), respectively. By increasing $\bar r$ or T if necessary, we may assume without loss of generality that $x_{\mathrm{s}} = T/\bar r^{\lambda}$. Next, for any $\delta < \bar r$, we define the open regions (see Figure 2)

$$K_\delta = \big\{(t,r)\,|\,0<t<T,\ \delta<r<\bar r,\ \tfrac{t}{r^\lambda} > x_{\mathrm{s}}\big\}$$

and

$$J_\delta = \big\{(t,r)\,|\,-T<t<T,\ \delta<r<\bar r,\ \tfrac{t}{r^\lambda} < x_{\mathrm{s}}\big\}.$$

We set

$$\begin{aligned} M(\psi) &:= \iint_{\mathbb{R}\times\mathbb{R}^+} (\rho\psi_t + \rho u\psi_r)\, r^m dr dt \\ &= \Big\{ \iint_{\mathbb{R}\times[0,\delta]} + \iint_{J_\delta} + \iint_{K_\delta} \Big\} (\rho\psi_t + \rho u\psi_r)\, r^m dr dt \\ &=: M_\delta(\psi) + \Big\{ \iint_{J_\delta} + \iint_{K_\delta} \Big\} (\rho\psi_t + \rho u\psi_r)\, r^m dr dt \end{aligned} \tag{5.6}$$

and

$$\begin{aligned} I(\theta) &:= \iint_{\mathbb{R}\times\mathbb{R}^+} \big(\rho u\theta_t + \rho u^2\theta_r + p\big(\theta_r + \tfrac{m\theta}{r}\big)\big)\, r^m dr dt \\ &= \Big\{ \iint_{\mathbb{R}\times[0,\delta]} + \iint_{J_\delta} + \iint_{K_\delta} \Big\} \big(\rho u\theta_t + \rho u^2\theta_r + p\big(\theta_r + \tfrac{m\theta}{r}\big)\big)\, r^m dr dt \\ &=: I_\delta(\theta) + \Big\{ \iint_{J_\delta} + \iint_{K_\delta} \Big\} \big(\rho u\theta_t + \rho u^2\theta_r + p\big(\theta_r + \tfrac{m\theta}{r}\big)\big)\, r^m dr dt. \end{aligned} \tag{5.7}$$

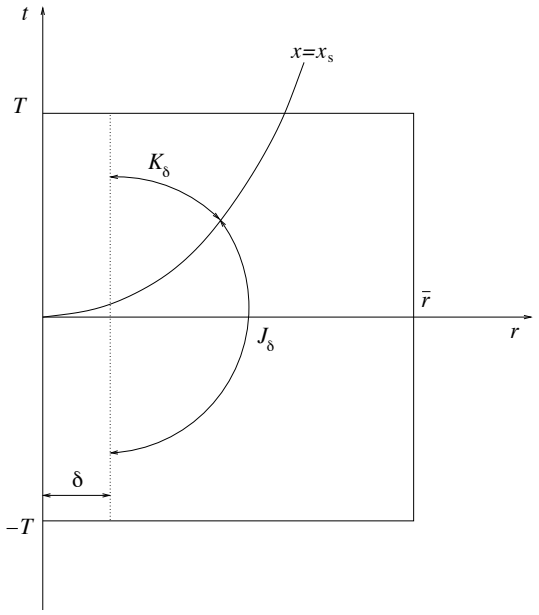

FIG. 2. *Regions of integration in the weak formulation.*

Part (iii) of Definition 5.3 amounts to the statement that $M(\psi)$ and $I(\theta)$ vanish. We establish this by showing that the right-hand sides of (5.6) and (5.7) tend to zero as $\delta \downarrow 0$. First, according to the continuity properties established in Proposition 4.8, the integrands in the expressions for $M(\psi)$ and $I(\theta)$ are all locally $r^m drdt$-integrable. It follows that both $M_\delta(\psi)$ and $I_\delta(\theta)$ tend to zero as $\delta \downarrow 0$. (For $I_\delta(\theta)$, we exploit that θ belongs to $C_0^1(\mathbb{R} \times \mathbb{R}_0^+)$; specifically, the function $\frac{m\theta}{r}$ is uniformly bounded.)

It remains to estimate the integrals over J_δ and K_δ in (5.6) and (5.7). For this, we use that (ρ, u), by construction, is a classical (Lipschitz continuous) solution of the isentropic Euler system (1.4)–(1.5) within each of the open regions J_δ and K_δ. Furthermore, the Rankine–Hugoniot relations (2.1) are satisfied across their common boundary along the curve $r = \mathcal{R}(t) = (\frac{t}{x_s})^{\frac{1}{\lambda}}$. Applying the divergence theorem to each region, we therefore have

$$\Big\{ \iint_{J_\delta} + \iint_{K_\delta} \Big\} \left(\rho\psi_t + \rho u \psi_r\right) r^m dr dt = \delta^m \int_{-T}^{T} (\rho u \psi)(t, \delta)\, dt \tag{5.8}$$

and

$$\Big\{ \iint_{J_\delta} + \iint_{K_\delta} \Big\} \left(\rho u \theta_t + \rho u^2 \theta_r + p\big(\theta_r + \tfrac{m\theta}{r}\big)\right) r^m dr dt = \delta^m \int_{-T}^{T} [(\rho u^2 + p)\theta](t, \delta)\, dt. \tag{5.9}$$

Using (1.8) and (1.10) and changing integration variable from t to x, we get for (5.8) that

$$\left| \delta^m \int_{-T}^{T} (\rho u \psi)(t, \delta)\, dt \right| \lesssim \delta^{n+\kappa} \left\{ \int_{-T/\delta^\lambda}^{-1} + \int_{-1}^{1} + \int_{1}^{T/\delta^\lambda} \right\} \left(\left| \tfrac{C(x)}{x} \right|^{\frac{2}{\gamma-1}} \left| \tfrac{V(x)}{x} \right| \right) dx,$$

where we have split up the x-integration into three parts (assuming that $\delta < T^{\frac{1}{\lambda}}$).

Making use of (4.24), we obtain that the three integrals add up to an $O(1)$ term, so that

$$\left|\delta^m \int_{-T}^{T} (\rho u \psi)(t,\delta)\, dt\right| \lesssim \delta^{n+\kappa}. \tag{5.10}$$

The condition that $n+\kappa > 0$ is equivalent to $\lambda < \lambda_0 := 1 + \frac{n}{2}(\gamma - 1)$. By construction, we have that $\lambda < \hat{\lambda} \leq \bar{\lambda}$. Also, it is immediate to verify that $\bar{\lambda} < \lambda_0$. It therefore follows from (5.10) that the right-hand side of (5.6) vanishes as $\delta \downarrow 0$ for all values of λ under consideration. This establishes the weak form of the mass equation (5.3).

We argue similarly for the momentum equation. From (1.8) and (1.10), changing integration variable from t to x, and using (4.24), we get for (5.9) that

$$\begin{aligned}
&\left|\delta^m \int_{-T}^{T} [(\rho u^2 + p)\theta](t,\delta)\, dt\right| \\
&\lesssim \delta^{m+\lambda+\kappa\gamma} \left\{ \int_{-T/\delta^\lambda}^{-1} + \int_{-1}^{1} + \int_{1}^{T/\delta^\lambda} \right\} \left(\left|\tfrac{C(x)}{x}\right|^{\frac{2}{\gamma-1}} \left|\tfrac{V(x)}{x}\right|^2 + \left|\tfrac{C(x)}{x}\right|^{\frac{2\gamma}{\gamma-1}} \right) dx \\
&\lesssim \delta^{m+\lambda+\kappa\gamma} \left(1 + \delta^{-\kappa\gamma-\lambda}\right) = \delta^{m+\kappa\gamma+\lambda} + \delta^m.
\end{aligned}$$

As $m + \lambda + \gamma\kappa > n + \gamma\kappa > 0$ (the latter inequality being equivalent to $\lambda < \bar{\lambda}$), we obtain from (5.9) that the right-hand side of (5.7) vanishes as $\delta \downarrow 0$. This establishes the weak form of the momentum equation (5.4). This concludes the proof that (ρ, u) satisfies part (iii) of Definition 5.3.

This establishes part (2) of the Main Result, concluding its demonstration.

6. Concluding remarks. The solutions constructed above have locally finite mass and energy; however, their total mass and energy are unbounded (e.g., (4.18) and the condition $n + \kappa > 0$ shows that $\int_0^\infty \rho(0,r) r^m\, dr = +\infty$). We shall argue that the blowup behavior exhibited by these solutions can occur also in the presence of finite mass and energy. For this it suffices to establish the following property of the constructed solutions: The 1-characteristics passing through the points on a curve $\{(r,t) \,|\, \frac{t}{r^\lambda} \equiv \bar{x}\}$, with $\bar{x} < 0$ and sufficiently small, all pass through points on the *strictly positive* r-axis at time $t = 0$. Indeed, we can fix any time $t_0 < 0$ and modify any one of the solutions described in the Main Result at time t_0 at locations $r > \bar{r}_0 := (\frac{t_0}{\bar{x}})^{\frac{1}{\lambda}}$. The modification can be made so as to give finite total mass and energy at time $t = 0$. Assuming for now that the stated property holds, there is an interval near the origin where the original solution remains unaffected by the modification, so that blowup still occurs in the modified solution. In this manner, we obtain initial data at time t_0 which leads to solutions exhibiting amplitude blowup at the origin as described in the Main Result and whose total mass and energy are finite.

To argue for the stated property, recall that the solutions $(V(x), C(x))$ of (1.17) used in the construction above are such that $\frac{V(x)}{x}$ and $\frac{C(x)}{x}$ approach finite, nonzero limits as $x \to 0$ (see section 4.3). There are therefore finite constants $A > 0$ and

$B < 0$ such that

$$0 < \tfrac{V(x)}{x} < A, \qquad B < \tfrac{C(x)}{x} < 0 \qquad \text{for } x_0 < x < 0,$$

where we recall that $(V(x_0), C(x_0)) = P_8$. Next, fix $\bar{x} \in (x_0, 0)$, let $(\bar{r}, \bar{t})$ be any point on the curve $\bar{X} := \{(r,t) \,|\, \frac{t}{r^\lambda} \equiv \bar{x}\}$, and let $\mathfrak{r}(t)$ be the 1-characteristic through $(\bar{r}, \bar{t})$. Since the constructed flow is continuous for negative times and since $\{(t,r) \,|\, \frac{t}{r^\lambda} \equiv x_0\}$ is a 1-characteristic (see section 4.3), it follows that the 1-characteristic $\mathfrak{r}(t)$ remains inside the region $\{(t,r) \,|\, x_0 < \frac{t}{r^\lambda} < 0\}$ for $t \in (\bar{t}, 0)$. Along $\mathfrak{r}(t)$, we therefore have

$$\dot{\mathfrak{r}}(t) = (u-c)|_{(t,\mathfrak{r}(t))} = \tfrac{\mathfrak{r}(t)^{1-\lambda}}{\lambda} \left(\tfrac{C(x)}{x} - \tfrac{V(x)}{x} \right) |_{x = \frac{t}{\mathfrak{r}(t)^\lambda}} > \tfrac{(B-A)}{\lambda} \mathfrak{r}(t)^{1-\lambda}.$$

Integrating from time $\bar{t}$ to time 0 yields $\mathfrak{r}(0)^\lambda > \bar{r}^\lambda (1 + (A-B)\bar{x})$. As $A - B > 0$, this shows that, for $\bar{x}$ sufficiently small (negative), we have $\mathfrak{r}(0) > 0$. Thus, all 1-characteristics through points along $\bar{X}$ cross the r-axis at time $t = 0$ at *strictly* positive locations.

Finally, a similar argument shows that the same property holds for the particle trajectories (i.e., solutions to $\dot{r} = u(t, r(t))$) through points along $\bar{X}$. This provides confirmation of the fact that there is no "accumulation of mass" at the origin; i.e., the density field never contains a Dirac distribution at the origin, including at time $t = 0$.

Acknowledgments. The authors are grateful to the anonymous referees whose constructive remarks improved the presentation.

REFERENCES

[1] S. Atzeni and J. Meyer-ter Vehn, *The Physics of Inertial Fusion*, Internat. Ser. Monogr. Phys. 125, Oxford University Press, Oxford, 2004.

[2] G.-Q. Chen and T.-H. Li, *Global entropy solutions in l^∞ to the Euler equations and Euler-Poisson equations for isothermal fluids with spherical symmetry*, Methods Appl. Anal., 10 (2003), pp. 215–243.

[3] G.-Q. G. Chen and M. Perepelitsa, *Vanishing viscosity solutions of the compressible Euler equations with spherical symmetry and large initial data*, Comm. Math. Phys., 338 (2015), pp. 771–800.

[4] G.-Q. G. Chen and M. R. I. Schrecker, *Vanishing viscosity approach to the compressible Euler equations for transonic nozzle and spherically symmetric flows*, Arch. Ration. Mech. Anal., 229 (2018), pp. 1239–1279, https://doi.org/10.1007/s00205-018-1239-z.

[5] R. Courant and K. O. Friedrichs, *Supersonic flow and shock waves*, Springer-Verlag, Berlin, 1976. Reprinting of the 1948 original; Applied Mathematical Sciences, Vol. 21.

[6] C. M. Dafermos, *Hyperbolic conservation laws in continuum physics*, Grundlehren Math. Wiss. 325 [Fundamental Principles of Mathematical Sciences], Springer-Verlag, Berlin, 4th ed., 2016, https://doi.org/10.1007/978-3-662-49451-6.

[7] J. Duderstadt and G. Moses, *Inertial Confinement Fusion*, Wiley, New York, 1982.

[8] G. Guderley, *Starke kugelige und zylindrische verdichtungsstösse in der nähe des kugelmittelpunktes bzw. der zylinderachse*, Luftfahrtforschung, 19 (1942), pp. 302–311.

[9] D. Hoff, *Spherically symmetric solutions of the Navier-Stokes equations for compressible, isothermal flow with large, discontinuous initial data*, Indiana Univ. Math. J., 41 (1992), pp. 1225–1302.

[10] H. K. Jenssen and C. Tsikkou, *On similarity flows for the compressible Euler system*, J. Math. Phys., 59 (2018), 121507, https://doi.org/10.1063/1.5049093.

[11] H. K. Jenssen and C. Tsikkou, *Multi-d isothermal Euler flow: Existence of unbounded radial similarity solutions*, Phys. D., 410 (2020), 132511, https://doi.org/10.1016/j.physd.2020.132511.

[12] R. B. Lazarus, *Self-similar solutions for converging shocks and collapsing cavities*, SIAM J. Numer. Anal., 18 (1981), pp. 316–371.

[13] S. Pfalzner, *An Introduction to Inertial Confinement Fusion*, Series in Plasma Physics, CRC Press, Boca Raton, FL, 2006.

[14] M. R. I. Schrecker, *Spherically symmetric solutions of the multidimensional, compressible, isentropic Euler equations*, Trans. Amer. Math. Soc., 373 (2020), pp. 727–746, https://doi.org/10.1090/tran/7980.

[15] L. I. Sedov, *Similarity and Dimensional Methods in Mechanics*, "Mir," Moscow, 1982. Translated from the Russian by V. I. Kisin.

[16] K. P. Stanyukovich, *Unsteady Motion of Continuous Media*, Translation edited by Maurice Holt; literal translation by J. George Adashko, Pergamon Press, New York, 1960.